Earth **Surface**
Dynamics
Discussions
EGU
Open Access

Rapid Holocene bedrock canyon incision of Beida River, North Qilian Shan, China

Yiran Wang[1], Michael E. Oskin[1], Youli Li[2], Huiping Zhang[3]

[1]Department of Earth and Planetary Sciences, University of California, Davis, California, USA
5 [2]College of Urban and Environmental Sciences, Peking University, Beijing, China
[2]Institute of Geology, China Earthquake Administration, Beijing, China

Correspondence to: Yiran Wang (yrwwang@ucdavis.edu)

Abstract. Located at the transition between monsoon and westerly dominated climate systems, major rivers draining the western North Qilian Shan incise deep, narrow canyons into latest Quaternary foreland basin sediments of the Hexi Corridor.

10 Field surveys show that the Beida River incised 125 m at the mountain front over the Late Pleistocene and Holocene at an average rate of 6 m/kyr. We hypothesize that a steep knickzone, with 3% slope, initiated at the mountain front and has since retreated to its present position, 10 km upstream. Terrace dating results suggest this knickzone formed around the mid-Holocene, over a duration of less than 1.5 kyr, during which incision accelerated to at least 25 m/kyr. These incision rates are much larger than the uplift rate across the North Qilian fault, which suggests a climate-related increase in discharge drove

15 rapid incision over the Holocene and formation of the knickzone. Using the relationship between incision rates and the amount of base level drop, we show the maximum duration of knickzone formation to be 700 yr and the minimum incision rate to be 50 m/kyr. This period of increased river incision is the result of increasing excess discharge, which likely corresponds to a pluvial lake-filling event at the terminus of the Beida River and correlates with a wet period driven by strengthening of the Southeast Asian Monsoon.

20 ## 1 Introduction

An incising river responds to tectonic or climatic perturbation by adjusting its slope, expressed by formation of knickpoints or knickzones (Crosby and Whipple, 2006; Tucker and Whipple, 2002; Whittaker, 2012), and through changes of its channel width (Finnegan et al., 2005). Understanding the evolution and migration of knickzones, channel width, and the coupling between these adjustments, is important in unravelling the type, duration, and amplitude of a perturbation (Attal et al., 2011;

25 Berlin and Anderson, 2007; Bishop et al., 2005). Previous studies on headward migrating knickpoints focus on the role of tectonic uplift or a base level fall, and usually regard climate conditions and channel width as constant (e.g. Tucker and Whipple, 2002; Crosby and Whipple, 2006; Haviv et al., 2006; Wobus et al., 2006). Here we present a case of steep, quickly retreating knickzones within the western North Qilian Shan, formed under the combined influence of climatic change and lithologic control. Through modelling of incision of the Beida River, as recorded by its profile and stream terraces preserved along its

30 course, we suggest this knickzone was formed during a short period, 4-5 thousand years before present, under an exceedingly

fast incision rate. This is most likely to be the result of an increase in river discharge, and perhaps a commensurate decrease of sediment supply.

In western China, the North Qilian Shan is the source of several northeast flowing rivers with deep canyons incised across the mountain-basin boundary (Figure 1). In the western North Qilian Shan, three major tributaries of the Hei He drainage, Maying,

35   Hongshuiba, and Beida River, carve deeply into the foreland sediments and across the fault-controlled boundary with the bedrock hinterland, forming prominent knickzones within the hinterland that are tens of meters high (Figure 2). As one of these deeply incised rivers, the Beida River is characterized by a prominent knickzone which separates its profile into three patches (upper patch 1, knickzone patch 2, and lower patch 3; Figure 3). Each patch can be distinguished by different channel slopes and channel widths: gentle and wide upper patch, steep and narrow knickzone, and a lower patch with a gentle slope

40   similar to the upper patch, but a narrower channel. The successive generation and retreat of these patches corresponds to different boundary conditions (cf. Royden and Perron, 2013), and together record the incision history at the mountain front.
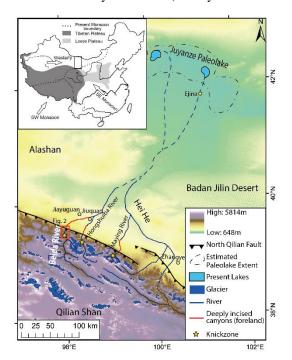

Figure 1 Digital elevation map of the research area and the Hei He drainage system. Glacial coverage mapped based on Raup et al., (2007). Inset figure: Location of our research area with respect to monsoon and westerly moisture sources.
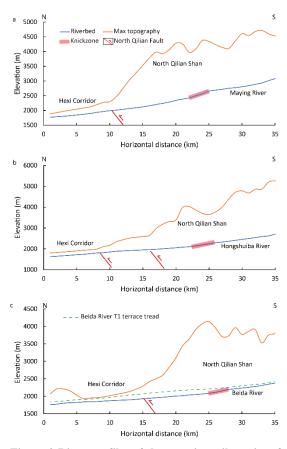
Figure 2 River profiles of three major tributaries of the Hei He drainage, and swath profiles of maximum topography the North Qilian Shan surrounding the rivers. Swaths are 16 km in width, centred on each river. Locations of active strands of the North Qilian fault denote foreland-hinterland junction at mountain front. All three rivers exhibit deep incision below the top of foreland-basin sediments. Red highlights knickzone reach within bedrock. Dashed line in C is reconstructed profile of the Beida River ca. ~24 ka, prior to onset of rapid incision phase.
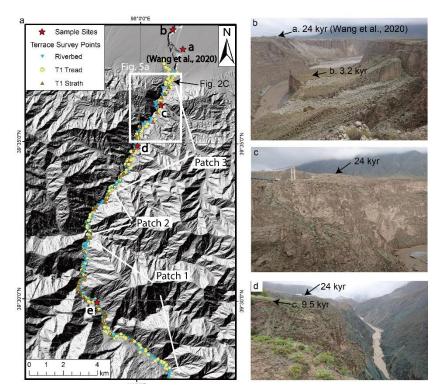
Figure 3 a) Map of the Beida River within the north Qilian Shan, with survey points and geochronology sample sites indicated. **b)** Photo of Beida River canyon and sample site a and b within the foreland, looking upstream. Thick layers of gravel are exposed on the canyon walls. **c)** Photo of Beida River canyon and T1 terraces near the mountain front, looking east (location in figure 2a). In this photo, the 24 kyr T1 terrace tread is ~40 m above the 9.5 kyr inset terrace tread. **d).** Photo of Beida River canyon and sample site c inside the mountains, looking upstream. This photo shows that the Beida River deeply incises into the bedrock below the terrace fill.

2 Geological background

The Qilian Shan form the northeastern margin and the youngest growing portion of the Tibetan plateau (Tapponnier et al., 2001). The Hexi Corridor, north of the Qilian Shan, consists of a chain of foreland basins. Bordering arid central Asia, Qilian Shan and Hexi Corridor occupy the transition zone between Southeast Asian Monsoon and westerlies (An et al., 2001; Wei and Gasse, 1999). The monsoon brings summer rain inland while the mid-latitude westerlies bring dry air and a small amount of water vapor in winter. The monsoon influence diminishes westward as the annual precipitation within the Hexi Corridor decreases from 300~400 mm in the east to <100 mm in the west (Meng et al., 2012). At high altitude within the Qilian Shan (> 4000 m), the precipitation is significantly greater, with an overall trend that also decreases presently from east (>700 mm) to west (~300 mm) (Shi et al., 2006). The modern glacial equilibrium line altitude of Qilian Shan increases from 4400 to 5000 m from northeast to southwest (Shi, 2011), reflecting the decrease in precipitation. Between the year 2005 to 2010, within the Qilian Shan there were 2684 glaciers with a total area of 1600 km^2 and an ice volume of 84 km^3 (Guo et al., 2014; Sun et al., 2015). These glaciers covered approximately 4% of the landscape above 4000 m elevation. The extent of these glaciers has

70 fluctuated repeatedly throughout the Quaternary. Dating of moraines suggests that glacial advances have occurred during the little ice age (~1300-1850 A.D.), MIS (Marine Isotope Stage) 2, MIS 4, MIS 6, and MIS 12; some glacial expansion may have occurred during MIS 3 as well (Shi et al., 2006).

The Hei He (river) forms the largest drainage basin in the North Qilian Shan, and terminates within the Juyanze paleolake basin, north of the Hexi Corridor. Sediment and core records from the Juyanze paleolake basin indicate frequent dry-wet

75 oscillations over the past 11,000 yr (Hartmann and Wünnemann, 2009; Herzschuh et al., 2004; Mischke et al., 2002, 2005). The highest lake level occurred during the early-Holocene (~20 m deep), and the highest mid-Holocene lake level (~15–17 m deep) occurred at about 4200 yr BP (East Juyanze lake, Hartmann and Wünnemann, 2009).

Three major tributaries, Beida, Hongshuiba, and Maying, join the Hei He from the south and west (Figure 1). In the hinterland, the three rivers flow through Pre-Cambrian and Paleozoic meta-sedimentary and meta-igneous rocks; in the foreland, these

80 rivers incise into Quaternary sediments of the Hexi Corridor. The North Qilian range overthrusts the southern margin of the Hexi Corridor, placing metasedimentary rocks against the Quaternary basin deposits. Presently, the channels of the Maying, Hongshiba, and Beida River each incise over 100m into Late Pleistocene alluvial fans of the foreland basin, and by a similar depth into correlative fill terraces within the range (Hetzel et al., 2019; Yang et al., 2020; Wang et al., 2020). A prominent knickzone occurs along each river, presently located ~10-15 km upstream of the mountain front (Figure 2).

85 As the largest tributary of the Hei He, the Beida River is ~360 km long, occupying 6880 km^2 drainage area within the Qilian Shan (Ding et al. 1999; Jiuquan History Compilation Committee, 1998). Along the Beida River, at least two generations of fill terraces (T1 and T2) are preserved well and continuously in the hinterland and extend to the foreland basin. Our previous research (Wang et al., 2020) suggests that T1 was abandoned at 24±3 kyr B.P., and T2 was abandoned at 144±30 kyr B.P. Flights of terraces inset below both main terrace treads, marking progressive degradation of the terrace fill and incision into

90 underlying bedrock. Along the mountain front, strands of the North Qilian fault cut the terraces of Beida River, offsetting T1 and T2 vertically by 14.8 m and >59.7 m, respectively. In the hinterland, the T2 terrace profile reveals a long wavelength fold (~30km) with maximum uplift of ~120 m relative to T1. Combined, the fault offset and folding indicate a maximum uplift rate of ~1 m/kyr at the fold crest, and a horizontal shortening rate of 1.4±0.4 m/kyr across the North Qilian Shan (Wang et al., 2020).

95 ## 3 Methods

3.1 Field survey

The late Pleistocene T1 fill terrace, up to 60 m thick, is preserved continuously along the narrow, lower bedrock gorge of the Beida River. This terrace grades to an extensive alluvial fan deposit emanating from the mountain front, with minor disruption from reverse fault offsets (Figure 1). The Beida river gorge cuts across the fault-controlled basin boundary, forming a narrow

100 slot canyon up to 125 m deep within the foreland-basin fan gravels. We mapped and surveyed the terrace sequence and the course of Beida River inside the mountain range using a laser rangefinder (~0.3 m distance accuracy, 0.25° inclination accuracy)
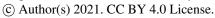
and differential GPS. Wherever possible, the terrace tread (top of the fluvial gravel), terrace strath (base of fluvial gravel), and present riverbed were measured together (Figure 3, Table S1). In the foreland, we extract terrace elevations and the river profile from an 8 m resolution digital elevation model, produced by the Polar Geospatial Center (Shean, 2017). Present bedrock
105 channel widths were measured from Google Earth imagery at 100 m intervals along the river course. We measured the width of the water surface from imagery acquired during the wet season, mostly between July to September, 2010 to 2016. Due to limited data availability, a few measurements were obtained from imagery acquired in May and October (Table S2).

3.2 Geochronology

The abandonment age of T1 was dated to be 24±3 kyr by combining optically stimulated luminescence (OSL) and Terrestrial
110 Cosmogenic Nuclide (^{10}Be) exposure ages (Figure 3 sample site a; Wang et al., 2020). To document the post-24 kyr incision history of Beida River, we collected charcoal samples from the fine sand and silty overbank deposits on three inset terraces (Figure 3 sample site c, d, e, Figure S2). These overbank deposits were deposited after terrace formation, but before incision was sufficient to isolate the terrace surface from flood events. An OSL sample (Figure 3 sample site b) was collected on an even lower insect terrace in the foreland basin from the bottom of the loess covering the terrace deposits. Ten charcoal samples
115 were measured at the Keck Carbon Cycle AMS Facility at UC Irvine. The results were calibrated with IntCal14 calibration curve (Reimer et al., 2013) (Table 1). The OSL sample (BD-O-12) was processed and measured at the State Key Laboratory of Earthquake Dynamics, China Earthquake Administration. The equivalent doses (De) for the pure fine-grained quartz were determined by the simplified multiple aliquot regenerative-dose (SMAR) protocol (Table 2, Table S3, Figure S1).

Table 1 ^{14}C age of Beida River terraces

Sample site	Coordinates	Sample name	fraction Modern	±	D^{14}C (‰)	±	^{14}C age (BP)	±	Calibrated age * 1σ (BP)	2σ
c	39.60126°, 98.01365°	BDC-3	0.3462	0.0028	-653.8	2.8	8520	70	9473-9544	9332-9340 9404-9632 9645-9657
		BDC-4	0.3393	0.0008	-660.7	0.8	8680	20	9557-9630 9647-9653	9552-9679
		BDC-5	0.3378	0.0008	-662.2	0.8	8720	20	9611-9699	9561-9737
		BDC-6	0.3320	0.0009	-668.0	0.9	8855	25	9895-9949 9990-10012 10025-10038 10061-10134	9784-9848 9861-9878 9883-9966 9982-10155

Earth **Surface**
Dynamics
Discussions
Open Access
EGU

d	39.57600°, 97.99493°	BDC-8	0.5973	0.0011	-402.7	1.1	4140	15	4617-4652 4669-4703 4757-4765 4784-4809	4580-4726 4752-4770 4780-4815
		BDC-9	0.5715	0.0011	-428.5	1.1	4495	20	5054-5077 5105-5136 5163-5189 5213-5228 5231-5251 5257-5281	5047-5147 5153-5202 5210-5288
		BDC-10	0.5862	0.0011	-413.8	1.1	4290	15	4844-4856	4839-4862
e	39.498771°, 97.971940°	BDC-11	0.4702	0.0012	-529.8	1.2	6060	20	6893-6944	6807-6811 6856-6979
		BDC-12	0.4497	0.0029	-550.3	2.9	6420	60	7309-7419	7185-7186 7246-7439
		BDC-14	0.4725	0.0010	-527.5	1.0	6025	20	6800-6815 6845-6901	6797-6934

120

Table 2 OSL age of loess covering terrace tread

Sample Site	Sample no.	Coordinates	U /ppm	Th /ppm	K (%)	Water Content (%)	Dose Rate (Gy/ka)	Equivalent Dose [1] (Gy)	Age [1] (ka)
b	BD-O-12	98.02299, 39.64376	2.34±0.10	9.32±0.28	1.67±0.06	0	3.5±0.3	11.4±0.7	3.2±0.2

1. Uncertainties in equivalent dose, dose rate and age determinations are expressed at the 1σ confidence level.

3.3 Bedrock incision model

125 We apply the concept of slope patches (Royden & Perron, 2013) to model the evolution of the Beida River stream profile. The formation of a slope patch is based on stream power, which has the form

$$\frac{dz}{dt} = K \left(\frac{QS}{W}\right)^n \qquad , \qquad (1)$$

where z is the channel elevation, t is time, A is drainage area, Q is river discharge, S is channel slope, W is channel width, and K and n are an empirical erosional efficiency and exponent, respectively (Tucker & Whipple, 2002; Whipple & Tucker, 1999).

130   A slope patch forms in the bedrock channel immediately upstream of the channel outlet, with channel slope that develops in balance with the rate of base-level fall. Setting $\frac{dz}{dt}$ to the incision rate, I, at the mountain front, we rearrange equation 1 to solve for this channel slope:

$$S = \left|\frac{dz}{dx}\right| = \left(\frac{I}{K}\right)^{\frac{1}{n}}\left(\frac{W}{Q}\right) \qquad (2)$$

During formation of a slope patch, river profile elevation is found by integrating equation 2 over its finite span x_b to x. For

135   the case of the Beida River, no major tributary enters along its lower 30 km long course; the drainage area of Beida River, measured from 30 m SRTM DEM, at the river outlet (mountain front) is $\sim 6.91 \times 10^9$ km2, while the drainage area above the knickzone is $\sim 6.84 \times 10^9$ km2, leading to a ignorable difference of $\sim 1\%$. Thus, we assume that Q does not vary spatially along the channel course:

$$z(x) = \left(\frac{I}{K}\right)^{\frac{1}{n}}\left(\frac{W}{Q}\right)(x - x_b) + z_b = S(x - x_b) + z_b \qquad (3)$$

140   where x_b and z_b are the horizontal position and elevation of the channel outlet, respectively.

We model the bedrock incision history of the Beida river as a consequence of varying discharge over time. Each slope patch along its course corresponds to a past discharge condition. Once formed, a slope patch behaves as a kinematic wave, retaining its gradient as it retreats upstream (Perron and Royden, 2013). The elevation of the (n-1)th slope patch (the patch formed one stage before present) may thus be cast as a function of its slope during formation, $S_{(n-1)}$ and an effective base-level elevation

145   $z_{b(n-1)}$ of the slope patch projected to the outlet position. This base level may be predicted by correcting the present base level elevation, z_b, by the difference in the amount of incision across neighboring patches n and n-1,

$$z_{b(n-1)} = z_b + (I_{n,j} - I_{n-1,j})t_j. \qquad (4)$$

$I_{n,j}$ is the incision rate of patch n, currently being formed during time interval t_j, directly upstream of the outlet. $I_{n-1,j}$ is the incision rate of patch n-1 during that time interval t_j. Note that because discharge has changed, the latter incision rate is different than the incision rate during formation of patch n-1 (i.e. faster for an increase in discharge). For the (n-2)th patch, the effective

150   base level contains two correction terms (see z_{b1}, z_{b2} of figure 4c),

$$z_{b(n-2)} = z_b + (I_{n,j} - I_{n-2,j})t_j + (I_{n-1,j-1} - I_{n-2,j-1})t_{j-1}. \qquad (5)$$

This may be generalized to additional slope patches, each corrected by the incision rate differences between patches. We apply equations 4 and 5, combined with the incision recorded in stream terraces adjacent to the Beida river, to constrain its incision-

155   rate history.

4 Results

4.1 Beida River patches and terraces

Presently, the 30 km reach of Beida River upstream of the mountain front is entirely contained within a bedrock channel. Channel slopes, measured directly from fitting the long profile, show a knickzone between 10 to 12 km upstream of the

160   mountain front. The knickzone divides the river profile into three patches: patch 1, upstream of the knickzone, with slope of 0.013; patch 2, the knickzone itself, with slope of 0.029; patch 3, below the knickzone with slope of 0.012. Channel width also varies along the course of the Beida River (Figure 4d). In patch 1, the channel width ranges between 14 to 140 m, with an average of 43 m; in patch 2, the channel width ranges between 8 to 29 m, with an average of 17 m; in patch 3, the channel width ranges between 14 to 70 m, with an average of 30 m (Figure 4d).

165   North of the mountain front, the T1 fill terrace merges into the extensive T1 alluvial fan. Within the mountain range, the T1 fill ranges from 60 to 80 m of thickness, and consists of unconsolidated medium to poorly sorted, well-rounded boulder-cobble conglomerate and sandy conglomerate. The lithology of the sediments mainly consists of quartzite, granite, slate, and limestone. T1 treads are very well preserved, only covered by 1~2 m loess cap except at tributary junctions, where alluvial fans are deposited upon the tread. The T1 tread presently lies ~125 m above present riverbed of patch 3 at the mountain front, and ~60

170   m above riverbed of patch 1. Bedrock below the T1 strath is exposed continuously for 30 km upstream of the mountain front. The most prominent inset terrace, T1', is preserved continuously at an elevation 10 to 15 m lower than T1 tread, both inside the mountain range and in the foreland basin. [14]C dating of charcoal samples at site c (Figure 3, 4a) indicates abandonment of T1' prior to 9.5 ± 0.16 kyr BP. Inside the mountain range, several levels of inset terraces are preserved along the river, generally between a few meters to ~40 m below the T1' tread, recording progressive incision of the Beida River. An inset terrace at site

175   e, situated 42 m above the present riverbed of patch 1, yielded an age of 6.9 ± 0.07 kyr. At site d, an inset terrace with tread elevated 90 m above the patch 3 riverbed yielded an age of 4.7 ± 0.12 kyr (Figure 3, 4a, Table 1). In the foreland, the river incised into the basin deposits. T1' and other minor inset terraces of T1 occur ~10-30 m below the T1 tread and 80-100 m above present river level. Terraces are absent between this elevation and ~30-40 m above the riverbed (Figure 4a, 4b). An OSL sample was collected from an inset terrace 2.5 km downstream of the mountain front, with its tread 37 m above the present

180   riverbed, yielding an age of 3.2 ± 0.20 kyr from the bottom of the loess cover (site b; Table 2). Notably, the difference in elevation and age of site b and d indicates a pulse of very rapid incision of 43 m in 1.5 ± 0.3 kyr, or an average of ~28 m/kyr, uncorrected for differential uplift between the two sites.
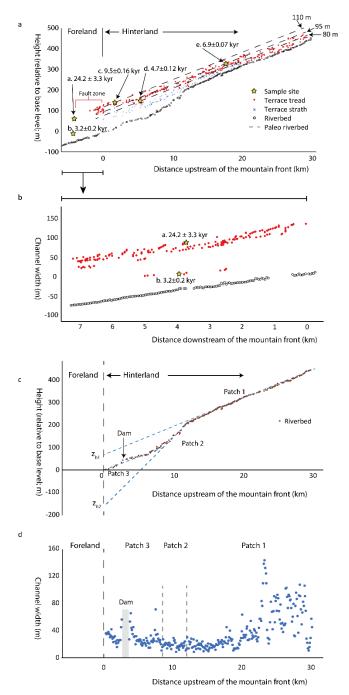
Figure 4 a) Longitudinal profile of the Beida River channel, terrace treads (T1 and all T1 inset terrace treads) and strath elevations,
185 **with sample sites and ages indicated. Dash lines are inferred prior river profiles corresponding to the sample site elevations, with**
the relative height above present base level annotated (not corrected for tectonic uplift). b) terrace elevations (red) and channel
elevations (open circles) along the Beida River within the foreland basin. Note sparse terrace record below T1/T1'. c) Three patches
of Beida river profile, projected to effective base level at the mountain front. d) Present bedrock channel width measured at 100m
intervals along the course of the Beida River. The width measurements that are within ~500 m upstream & downstream of the dam
190 **are excluded.**

10

4.2 Exposure of T1 bedrock strath

Though the terrace fill underlying the T1 tread is up to ~60-80 m thick, we find that the Beida river has not re-excavated its former channel. Instead, the river incised primarily along the western edge of its former canyon, and the paleocanyon fill and former walls of its bedrock gorge are preserved beneath the T1 fill deposit along much of the river course we surveyed (Figure
195   5, S3). Thus, bedrock incision likely commenced very soon after the onset of incision of T1. This is most clear for the ~3-4 km long reach immediately upstream of the North Qilian fault, where the wide T1 terrace treads (24 kyr) and T1' terrace tread (9.5 kyr) are preserved on the east bank of the Beida River, while only bedrock is exposed on the west bank. Farther upstream, exposures at several locations show that entire paleo-channel has been preserved beneath T1 and T1'. Our surveys further show that all observed terrace straths are located immediately beneath the prominent 9.5 kyr T1' terrace (Figure 4a). Therefore,
200   though it is difficult to pinpoint the exact starting time of the bedrock incision, based on the terrace distribution and bedrock exposure along the channel, we suggest that the onset of bedrock incision along the Beida River may have started as early as ~9.5 kyr B.P, the age of the inset T1' terrace.
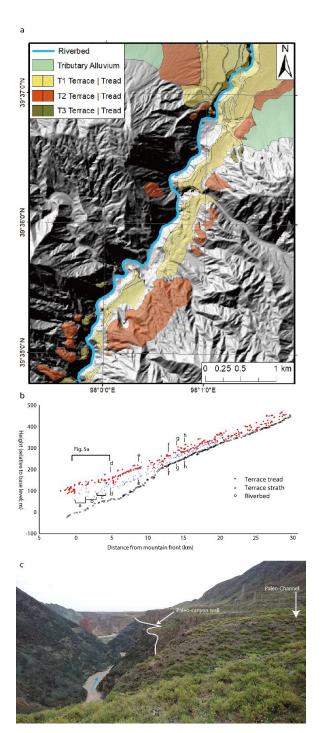
**Figure 5 Bedrock incision and terrace preservation along the Beida River. a. Terrace map of the lower reach of Beida River. T1
terraces are all preserved on the east side of the canyon. b. Terrace profiles of Beida River. Letters correspond to reaches where
terrace mapping indicates that the original paleocanyon is preserved and the river incised into the adjacent bedrock soon after the
abandonment of T1' (See Figure S3). c. Photo of the lower reach of Beida River, looking downstream, with paleochannel axis and
paleo-canyon wall annotated. Here the river incised mostly into bedrock along the west edge of the T1 terrace fill deposit.**

4.3 Incision rate estimation with terrace records

210   The incision rate at the mountain front for each stage may be calculated from the ages and relative heights of the T1 inset terraces. Because the sample sites are scattered along the river, the heights of these terraces cannot be compared directly. Instead, we reconstruct the elevation of the river channel at 9.5, 6.9, and 4.7 kyr B.P., by projecting the paleo channel through the three sample sites to the mountain front based on the slope of patch 1 (Figure 4a). The heights of these paleo channels above present riverbed at the mountain front are 110 m, 96 m, 80 m, respectively (Table 3). After correction for faulting at the

215   mountain front and folding of the range interior (Wang et al. 2020), the elevations without tectonic uplift at the mountain front are 102 m, 89 m, and 75 m above present base level, respectively (Table 3). The oldest T1 terrace (24.2 kyr) and the youngest terrace (3.2 kyr), 115 m and 37 m above the riverbed, are located on the footwall of the North Qilian Fault, therefore no adjustment for tectonic uplift is needed. With these adjusted terrace heights, we calculate the incision rate at mountain front between 24.2 to 9.5 kyr B.P. was ~0.9 m/kyr. Incision rate accelerated over much of the Holocene, from ~5 m/kyr between

220   9.5 to 6.9 kyr B.P. to ~6 m/kyr between 6.9 to 4.7 kyr B.P., to ~25 m/kyr, between 4. 7 to 3. 2 kyr B. P. The incision rate remains high, at ~25 m/kyr, from 3.2 kyr B. P. to present.

5 Discussion

5.1 Beida River knickzone formation and incision stages.

We rule out the possibility of tectonic uplift as a driver of the formation of the prominent knickzone (patch 2), for two reasons.

225   First, we document that the knickzone was formed after the abandonment of T1 and T1', and that this knickzone was cut largely within a newly formed bedrock channel, and not within re-excavated paleo-channel fill (Figure 4a). Therefore, it is unlikely that the knickzone formed by re-excavation of an older bedrock channel with a pre-existing knickzone that may have formed over a protracted period of uplift. Second, the rate of incision of the Beida River greatly exceeds the tectonic uplift rate. Based on our previous research (Wang et al., 2020), the average vertical uplift rate at the mountain front is only ~0.6

230   m/kyr. Additional uplift occurs via folding within the hinterland, reaching a maximum of ~15 m for the T1 terrace (vertical displacement by the frontal fault excluded) at 5 to 10 km upstream of the range front. This folding contributes an additional ~0.6 m/kyr to the uplift rate. Compared to the ~12 m/kyr post 9.5 kyr B.P. average river incision rate, the tectonic uplift rate is an order of magnitude less. This suggests that the Beida River profile is and has been in a transient state since 9.5 kyr B.P. An alternative hypothesis is that the Beida River knickzone formed in place, related either to a change in erodibility of bedrock

235   or a major tributary confluence. Based on a drainage-area analysis, no major tributary confluence occurs at the knickzone location. In the neighbouring Maying and Hongshuiba River, similar to the Beida River, present river channels also incised into Late Pleistocene fill terraces (22.5-26 kyr for Hongshuiba River, Hetzel et al., 2019, Yang et al., 2020), forming prominent knickzones 10-15 km upstream of the mountain front (Figure 2). This suggests these knickzones share similar origins, reflecting regional forcing. Local variations of lithology would thus be an unlikely cause for knickzone formation. In addition,

240   if the knickzone of the Beida River were a persistent feature of the channel, evidence should be preserved in the strath (paleo river bed) elevations beneath the T1 terrace. We find that T1 strath elevations shows no such sign of a knickzone (Figure 4a). Therefore, neither the regional context nor local incision history suggest the presence of fixed knickzone, and this alternative hypothesis can be ruled out.

We interpret the knickzone of the Beida River as a migrating kinematic wave, related to an accelerated incision rate earlier in
245   time and downstream of its present position. We suggest Beida River knickzone formed in response to an abrupt change in the rate of base-level lowering (Whipple and Tucker, 1999). It is likely that knickzone of the Beida River first formed at the mountain front, where bedrock is juxtaposed against Quaternary foreland-basin sediments by the North Qilian fault. The knickzone is hypothesized to have formed here as a response to increased incision rate into the foreland-basin sediments, thus lowering base level relative to the bedrock. The most likely cause for this increase in incision rate is a change in river hydrology
250   during this time period, with perhaps a contribution from decreased sediment flux. Both mechanisms would increase transport capacity and promote incision of the unconsolidated foreland-basin sediments. By happenstance, it appears, the Beida River incised the western edge of its channel that was filled by T1. This brought the river channel in contact with bedrock well above its former channel thalweg position below T1. This resulted in formation of a knickzone as incision of the foreland basin outpaced bedrock incision upstream of the mountain front.

255   Based on the slope patch theory for bedrock incision, we associate the three slope patches along the bedrock channel of the Beida River as formed during three incision stages since 9.5 kyr B.P.. Each patch is tied to the mountain front outlet where the bedrock channel transitions to an alluvial channel. During the 1st stage, relatively slow incision rate in the foreland formed the gentle slope and wide channel of patch 1. During the 2nd stage, incision rate increased in the foreland, which leads to the formation of a steeper, narrower patch 2. During the 3rd stage, incision rate in the foreland decreased, therefore the youngest
260   patch 3 with gentle slope and wider channel formed, while the steeper patch 2 retreated upstream, replacing patch 1 (Figure 6). Combined with the terrace records, we therefore define the 1st incision stage to occur from 9.5 kyr to sometime around or after 4.7 kyr B. P., because the incision rates between 9.5 to 6.9 kyr B.P. and 6.9 to 4.7 kyr B.P. are identical within error, between ~5-6 m/kyr (Figure 7). This is followed by the 2nd stage, with an incision rate of at least ~25m/kyr. The 3rd, present stage, started after 3.2 kyr B.P. with an incision rate of ~12 m/kyr. In addition to our terrace chronology, this incision history
265   is also supported by the relative preservation of terraces along the Beida River, with a notable absence of terraces preserved between 40 and 80 m above river level (75 and 30 m below T1) within the foreland, during the period of most rapid incision inferred from the bracketing terrace record. Because the starting time and the duration of stage 2 is not well constrained due to the sparse terrace record, it is possible that stage 2 was shorter duration than 1.5 kyr and its ~25 m/kyr incision rate a minimum.
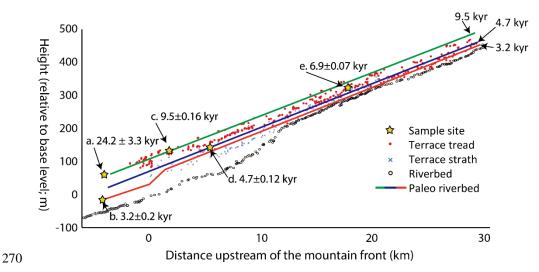
Figure 6 Simplified model for Beida River incision since 9.5 kyr. The surveyed terrace treads and the paleo riverbeds we projected are corrected for tectonic uplift, therefore slightly deviated from the sample locations. The time period between 24.2 to 9.5 kyr B.P. is not included in this model because the river was mostly incising into the T1 terrace fill, and therefore the incision of the foreland and hinterland should be synchronous.

Table 3 Terrace ages and relative heights.

Terrace Age (kyr)	Original terrace height (projected to mountain front, m)	Tectonic uplift rate[1]	Terrace Height (Adjusted based on tectonic uplift)	
			Relative to present riverbed at mountain front (m)	Relative to patch 1 (m)
24.2 ± 3.3	115 ± 3	0	115 ± 3	63 ± 3
9.5 ± 0.16	110 ± 2.7	0.86 ± 0.24	102 ± 5	50 ± 5
6.9 ± 0.07	96 ± 3.2	0.92 ± 0.25	89 ± 4.9	37 ± 5
4.7 ± 0.12	80 ± 2.4	1.08 ± 0.29	75 ± 3.8	23 ± 3.8
3.2 ± 0.2	37 ± 3	0	37 ± 3	-

[1] Tectonic uplift rate at the sample site is calculated based on the folding and faulting data in Wang et al., (2020).
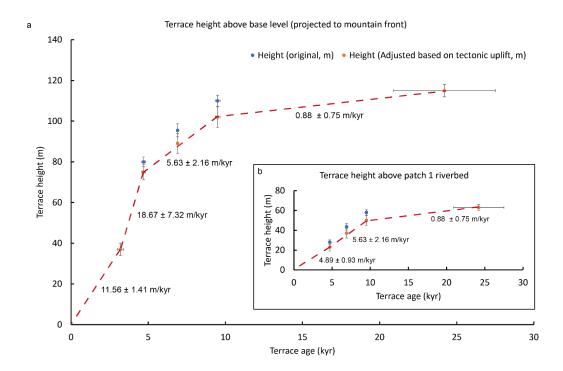
15

Figure 7 a) Terrace height above base level and the incision rate of each stage at the mountain front. b) Terrace height and incision rate of each stage above patch 1, upstream of the knickpoint. Details of elevations with correction for tectonic uplift are in Table 3.

5.2 Coupled incision model for knickzone formation

Geometric and timing relations for patches 1, 2, and 3 may be coupled to further constrain the duration and incision rate of the knickzone formation stage (stage 2). Here we formulate these relationships into two sets of constraints. Constraint 1 comes from the knickzone retreat process and the geometric relationship between patch 2 and 3. The effective base level of patch 2 (z_{b2}, Figure 4c) is determined by the relative incision rate between patch 2 and patch 3, and the duration of the 3rd stage. Based on equation 4, we have

$$z_{b2} = (I_3 - I_{2,3}) \times t_3 \qquad (6a)$$

Because we may estimate I_3 and t_3 from the position of the youngest, 3.2 kyr B.P. terrace, and z_{b2} from projection of the patch 2 river profile to the mountain front, we may calculate the incision rate along patch 2 during stage 3, $I_{2,3}$ as

$$I_{2,3} = I_3 - Z_{b2}/t_3 \qquad (6b)$$

It is reasonable to assume that during the knickzone formation, the incision rate along patch 2 should be greater than present incision rate, $I_2 > I_{2,3}$. With known I_3, t_3, and z_{b2} (see table S4 for details), the minimum rate of incision during knickpoint formation, I_2, is 50 ± 17 m/kyr.

To find the maximum duration for the time of knickpoint formation, t_2, we introduce a second set of constraints, derived from the total incision at the mountain front since 9.5 kyr B.P. and the total incision along patch 1 since 6.9 kyr should both match the observed terrace record:

$$H_{9.5kyr} = t_1 \times I_1 + t_2 \times I_2 + t_3 \times I_3 = I_1(9.5 \; kyr - t_2 - t_3) + I_2 t_2 + I_3 t_3 \qquad (7)$$

and

$$H_{6.9kyr} = I_1(6.9kyr - t_2 - t_3)I_1 + I_{1,2}t_2 + I_{1,3}t_3 \qquad (8)$$

In addition, the geometric relationship between patch 1 and 2 should also be satisfied. The effective base level of patch 1 (z_{b1}) is determined by the relative incision rate between patch 1 and patch 2, and patch 1 and patch 3, and the durations of the 2nd and 3rd stage. Based on equation 5, we have

$$z_{b1} = (I_2 - I_{1,2})t_2 + (I_3 - I_{1,3})t_3 \qquad (9)$$

Based on constraint 2 and $I_{2min}=50 \pm 17$ m/kyr, we calculate the maximum duration of the 2nd stage as 700 ± 340 yr, which is at approximately half of the duration suggested by isolated terrace record.

5.3 Channel width and bedrock incision rate

Variations in channel width may exert as much influence as discharge on incision rate (Lave and Avuoac, 2000). Drainage area, and thus discharge does not appreciably change across our research area, however the bedrock channel width varies widely, from over 100 m (patch 1) to as low as ~10 m (patch 2). Based on bedrock channel erosional mechanisms, the channel width should scale with discharge and channel slope (Finnegan et al., 2005, 2007; Lamb et al., 2015; Turowski et al., 2007; Wobus et al., 2006; Wohl and David, 2008). Though the narrowing of patch 2, and a clear, almost factor of two increase in the average width from patch 2 to patch 3 is consistent with coupling of channel width and slope, it is obvious that the upper reach of the patch 1 is considerably wider than expected (Figure 4d). In addition, the cause for narrowing of channel width on patch 1, a 5 km reach upstream of the knickzone, is also not clear. Increased flow velocity and shear stress immediately above the knickzone (Haviv et al., 2006) could contribute to this narrowing, though it is unlikely that such a hydraulic effect would extend for kilometers upstream. Another possibility is that the wider reach of the Beida River is a result of lateral incision and removal of a more extensive T1 terrace fill. Though bedrock is exposed in the channel throughout patch 1, T1 terraces more extensively preserved along its widest reach.

Variations in channel width could help to explain the two-fold difference in incision rate between patch 3 and patch 1 (Figure 7) at almost identical channel slopes (Figure 4). The narrower average width of patch 3 focuses stream power and enhances incision rate relative to patch 1 (Eq. 1). This explanation is at odds, however, with the presence of the narrow, downstream reach of patch 1, which by this reasoning should be incising as fast as patch 3. We speculate that this reach could reflect recent removal of the T1 terrace and focusing of the channel as it inset into bedrock. We note that the channel slope here is slightly steeper than upstream, which could indicate acceleration of incision rate. At present the terrace record is insufficient to test this hypothesis.

5.4 Possible causes of rapid incision of Beida River

Moderately fast incision of the Beida River since 9.5 kyr B.P. was punctuated by a < 700±340 yr event, during which the gorge incised ~30-40 m. This seems to be a unique event triggered by a short-term hydrologic perturbation. Similar knickzones are found in other western North Qilian rivers, i.e., Hongshuiba River and Maying River (Figure 1, 2), suggesting that this was a regional event that affected the entire western North Qilian Shan.

Formation of knickzones at the bedrock-basin boundary via an increase in incision rate into the foreland basin sediments requires an increase in water discharge or a decrease in sediment flux from upstream, either of which promotes an increase of available sediment-transport capacity (excess discharge). Decrease in sediment flux could be either due to glacial retreat and reduction of glacially produced sediment supply, or due to stabilization of hillslopes due to increased vegetation coverage inside the North Qilian Shan. Both explanations could help to explain the transition from infill to incision of the T1 terrace. But neither explanation seems likely to explain the short-term pulse of incision during stage 2.

One source of increasing water discharge during knickzone formation could have been glacial melt. Such a cause would increase discharge simultaneously for other rivers draining the glaciated highlands of the North Qilian Shan that display similar deep canyons and migrating knickpoints (Figure 1). However, present glacier coverage and discharge from the Beida River show that this explanation to be unlikely. The present ice cover and volume of Beida River drainage are 215.27 km^2 and 8.75 km^3, respectively (Sun et al., 2015). With the present average annual discharge of Beida River, 0.64 km^3 (Ding et al., 1999), a 50% increase of discharge due to excess glacial melt would deplete stored glacial ice in merely 27 yrs. In fact, due to rising temperature, the glacial coverage of Beida River drainage has shrunken at a pace of approximately 9% per decade over the past 50 yrs (Sun et al., 2015), contributing 15% of the average discharge of Beida River. Another study on a glacier west of the Beida River drainage indicates that during Last Glacial Maximum, the paleo-glacier cover was only 34% larger than the contemporary glacier cover (Hu et al., 2014). Combining all the evidence, we suggest increasing glacial melt may have played a role but alone it is not enough to trigger a dramatic knickzone formation event in the Beida River.

The other likely source of increasing water discharge is increasing precipitation, which could also affect neighbouring rivers. Compared to the glacial melt, precipitation has the potential of increasing water discharge to a higher level, especially in the arid-semi arid region like the North Qilian Shan. Lake records of the terminal Juyanze paleo-lake suggest the highest mid-Holocene lake level appeared at 4.2 kyr B.P. (Hartmann and Wünnemann, 2009), and pollen records of the same area suggest a wet, or pluvial period between 5.4 and 3.9 kyr B.P. (Herzschuh et al., 2004). This timing correlates well with knickzone formation during our 2nd stage. Regionally, evidence for similar humid periods can also be found from Zhuyeze, a lake fed by Shiyang River of the eastern North Qilian Shan (Chen et al., 2006), Qinghai Lake (Chen et al., 2016) located within the southeast Qilian Shan, Tianchi Lake of Liupan Shan (Zhou et al., 2010), and Yanhaizi Lake of Inner Mongolia (Chen et al., 2003). Cave records from upper Hanjiang region and Qinling Mountains (Tan et al., 2018) and stratigraphic sections from Loess Plateau also support the existence of a mid-Holocene humid period (Fang et al., 1999; Fang et al., 2003; Chen et al., 1997; Xiao et al., 2002).

Combining all evidence from river incision rates, glacial coverage, and local and regional climate records, we suggest that the brief, rapid incision event recorded by the Beida River knickzone is most likely linked to a pluvial event that resulted from an

360 increase of precipitation and possibly increased glacier melt during the mid-Holocene. The Qilian Shan and Hexi Corridor occupy the transitional zone between the Southeast Asian monsoon and the westerlies, with wet periods corresponding to increased monsoon influence (Tan et al., 2018). The combination of circumstantial evidence documented here suggests that a pluvial event occurred at the peak of monsoon influence within the westernmost North Qilian Shan. Between 24 kyr and 9.5 kyr B.P., the Beida River drainage was under the dominant influence of the arid westerly moisture source. Its incision rate

365 (corrected for uplift) of 0.9±0.8 m/kyr was more or less in balance with the rock uplift rate. During the Early Holocene, the humid Asian monsoon expanded to the central North Qilian Shan, where it affected the Hei He main stem and filled Juyanze lake to its highest lake level. The expanded monsoon may have mildly influenced the western North Qilian Shan, as it correlates to the 1st incision stage of the Beida River when the canyon incised at a rate of 5.6±2.2 m/kyr. During the mid-Holocene, the Asian monsoon grew stronger, starting in the Hei He drainage around 5.4 to 5.1 kyr B.P., and then expanding further to the

370 western North Qilian Shan a few hundred years later. This peak of monsoon influence lasted less than 700±340 yr, which led to an increase of precipitation therefore an increase of water discharge and incision rate. This climate event led to deepening of canyons into the foreland basin, prompting the formation of bedrock knickzones in the Maying, Hongshuiba, and Beida River sub-basins of the Hei He. During this pluvial period, the incision rate of the Bieda River increased to at least 50±17 m/kyr. Afterward, the discharge decreased to its present condition and river incision slowed to 11.6±1.4 m/kyr (Figure 8).
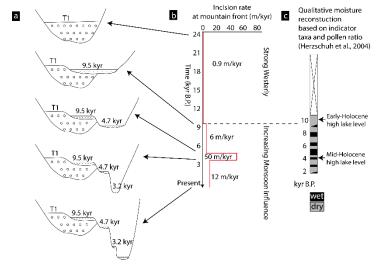

Figure 8 a) Schematic cross sections of Beida River channel evolution at the mountain front; b) diagram of incision rate vs. time since 24 kyr B.P.; c) climate reconstruction based on the Eastern Juyan palaeo-lake record (Herzschuh et al., 2004).

5.5 Glacial cycles and terrace formation in the North Qilian Shan

Though this study mainly focuses on the Holocene incision history of the Beida River, older fill terraces preserved within the

380 North Qilian Shan suggest there are at least two other fill-cut cycles that predate the latest Late Pleistocene-Holocene cycle.

Based on our prior fieldwork (Wang et al., 2020), there are two older generations correspond to fill terraces T2 and T3 (Figure 5a). T3 is undated, and only preserved in a few locations. [10]Be and OSL dating of T2 terrace tread suggests an age of ~144 kyr (Wang et al., 2020), which indicates the abandonment of T2 occurred during the penultimate glacial period, similar to that T1 was abandoned during the last glacial period. This suggests that the incision and deposition of fill terraces of Beida River

385 correlates with the glacial-interglacial cycles. A similar pattern occurs along the Hongshuiba River, the next major river to the east of the Beida River. The T1 terrace here is similar in age as T1 at the Beida River (26 kyr in Yang et al., 2020; 22.5 kyr in Hetzel et al., 2019), and the T4 terrace here has similar age as T2 terrace at the Beida River (153 kyr in Hetzel et al., 2019). In the eastern North Qilian Shan, terrace records of Shagou River also show a fill-cut pattern synchronized to glacial-interglacial cycles (Pan et al., 2003).

390 Therefore, we suggest the formation of fill terraces of different rivers along the North Qilian Shan is controlled by the same mechanisms, linked to glacial-interglacial cycles. In the Beida River, a full fill-cut cycle begins with the river backfilling its canyon with sediment during the glacial period. This is a period with elevated, glacially derived sediment flux, and perhaps lower discharge than at present. At the glacial-interglacial transition, the river transitions from deposition to erosion as sediment supply is gradually depleted. Fast incision commences during the early interglacial period as a result an increase of discharge

395 from the introduction of monsoon-derived summer moisture.

6 Conclusions

The Beida River in the North Qilian Shan has incised deeply into both the bedrock and the adjacent foreland basin sediments. The incision rates indicated from terrace records and our models greatly exceed rates of tectonic uplift here. Our work

400 demonstrates the capability of bedrock rivers in arid regions to incise deep channels and form fast retreating knickpoints within a short period. Field investigation and geomorphic mapping identify a 24 kyr fill terrace, T1, and several sets of inset terraces below. The longitudinal profile of the present river channel preserves a steep knickzone, located 10 to 12 km upstream of the mountain front. Terrace ages, and relationships between terrace treads and the riverbed, indicate that the knickzone was formed quickly after 5 kyr BP, driven by an increase of river discharge. By applying the concept of slope patches along with channel

405 geometry and terrace records, we constrain that during the knickzone formation, the incision rate was at least 50 ± 17 m/kyr and the duration of this period of increased discharge was less than 700 ± 340 yr, which is about half of that estimated from the sparse terrace age record alone. The period of increased incision identified from the Beida River correlates to a pluvial period recorded at the terminal Juyanze lake. The likely cause of rapid incision of the Beida River, and adjacent rivers with similar deeply incised canyons, is the increased influence of the southeast Asian Monsoon over the Holocene, with the most rapid

410 incision period corresponding to a peak of monsoon influence ca. 4 to 5 kyr B.P.

Acknowledgments, Samples, and Data

References

An, Z., Kutzbach, J. E., Prell, W. L. and Porter, S. C.: Evolution of Asian monsoons and phased uplift of the Himalaya - Tibetan plateau since Late Miocene times, Nature, 411(6833), 62–66, doi:10.1038/35075035, 2001.

Attal, M., Cowie, P. A., Whittaker, A. C., Hobley, D., Tucker, G. E. and Roberts, G. P.: Testing fluvial erosion models using the transient response of bedrock rivers to tectonic forcing in the Apennines, Italy, J. Geophys. Res. Earth Surf., 116(2), 1–17, doi:10.1029/2010JF001875, 2011.

Berlin, M. M. and Anderson, R. S.: Modeling of knickpoint retreat on the Roan Plateau, western Colorado, J. Geophys. Res. Earth Surf., 112(3), 1–16, doi:10.1029/2006JF000553, 2007.

Bishop, P., Hoey, T. B., Jansen, J. D. and Lexartza Artza, I.: Knickpoint recession rate and catchment area: The case of uplifted rivers in Eastern Scotland, Earth Surf. Process. Landforms, 30(6), 767–778, doi:10.1002/esp.1191, 2005.

Chen, C. T. A., Lan, H. C., Lou, J. Y. and Chen, Y. C.: The dry Holocene Megathermal in Inner Mongolia, Palaeogeogr. Palaeoclimatol. Palaeoecol., 193(2), 181–200, doi:10.1016/S0031-0182(03)00225-6, 2003.

Chen, F., Bloemendal, J., Wang, J. M., Li, J. J. and Oldfield, F.: High-resolution multi-proxy climate records from Chinese Loess: Evidence for rapid climatic changes over the last 75 kyr, Palaeogeogr. Palaeoclimatol. Palaeoecol., 130(1–4), 323–335, doi:10.1016/S0031-0182(96)00149-6, 1997.

Chen, F., Cheng, B., Zhao, Y., Zhu, Y. and Madsen, D. B.: Holocene environmental change inferred from a high-resolution pollen record, Lake Zhuyeze, arid China, Holocene, 16(5), 675–684, doi:10.1191/0959683606hl951rp, 2006.

Chen, F., Wu, D., Chen, J., Zhou, A., Yu, J., Shen, J., Wang, S. and Huang, X.: Holocene moisture and East Asian summer monsoon evolution in the northeastern Tibetan Plateau recorded by Lake Qinghai and its environs: A review of conflicting proxies, Quat. Sci. Rev., 154, 111–129, doi:10.1016/j.quascirev.2016.10.021, 2016.

Jiuquan History Compilation Committee: Jiuquan City Chorography, Lanzhou University Press, Lanzhou., 1998.

Crosby, B. T. and Whipple, K. X.: Knickpoint initiation and distribution within fluvial networks: 236 waterfalls in the Waipaoa River, North Island, New Zealand, Geomorphology, 82(1–2), 16–38, doi:10.1016/j.geomorph.2005.08.023, 2006.

Ding, Y., Ye, B. and Liu, S.: Effect of Climatic Factors on Streamf low in the Alpine Catchmen t of the Qilian Mountains, Acta Geol. Sin., 54(5), 431–437, 1999.

Fang, X., Lü, L., Mason, J. A., Yang, S., An, Z., Li, J. and Zhilong, G.: Pedogenic response to millennial summer monsoon
445 enhancements on the Tibetan Plateau, Quat. Int., 106–107, 79–88, doi:10.1016/S1040-6182(02)00163-5, 2003.

Fang, X. M., Ono, Y., Fukusawa, H., Bao-Tian, P., Li, J. J., Dong-Hong, G., Oi, K., Tsukamoto, S., Torii, M. and Mishima,
T.: Asian summer monsoon instability during the past 60,000 years: Magnetic susceptibility and pedogenic evidence from the
western Chinese Loess Plateau, Earth Planet. Sci. Lett., 168(3–4), 219–232, doi:10.1016/S0012-821X(99)00053-9, 1999.

Finnegan, N. J., Roe, G., Montgomery, D. R. and Hallet, B.: Controls on the channel width of rivers: Implications for modeling
450 fluvial incision of bedrock, Geology, 33(3), 229–232, doi:10.1130/G21171.1, 2005.

Finnegan, N. J., Sklar, L. S. and Fuller, T. K.: Interplay of sediment supply, river incision, and channel morphology revealed
by the transient evolution of an experimental bedrock channel, J. Geophys. Res. Earth Surf., 112(3),
doi:10.1029/2006JF000569, 2007.

Guo, W., Xu, J., Liu, S., Shangguan, D., Wu, L., Yao, X., ZHAO, J., LIU, Q., JIANG, Z., LI, P., WEI, J., BAO, W., YU, P.,
455 DING, L., LI, G., GE, C. and WANG, Y.: The Second Glacier Inventory Dataset of China (Version 1.0), Cold Arid Reg. Sci.
Data Cent. Lanzhou, doi:10.3972/glacier.001.2013.db, 2014.

Hartmann, K. and Wünnemann, B.: Hydrological changes and Holocene climate variations in NW China, inferred from lake
sediments of Juyanze palaeolake by factor analyses, Quat. Int., 194(1–2), 28–44, doi:10.1016/j.quaint.2007.06.037, 2009.

Haviv, I., Enzel, Y., Whipple, K. X., Zilberman, E., Stone, J., Matmon, A. and Fifield, L. K.: Amplified erosion above
460 waterfalls and oversteepened bedrock reaches, J. Geophys. Res. Earth Surf., 111(4), 1–11, doi:10.1029/2006JF000461, 2006.

Herzschuh, U., Tarasov, P., Wünnemann, B. and Hartmann, K.: Holocene vegetation and climate of the Alashan Plateau, NW
China, reconstructed from pollen data, Palaeogeogr. Palaeoclimatol. Palaeoecol., 211(1–2), 1–17,
doi:10.1016/j.palaeo.2004.04.001, 2004.

Hetzel, R., Hampel, A., Gebbeken, P., Xu, Q. and Gold, R. D.: A constant slip rate for the western Qilian Shan frontal thrust
465 during the last 200 ka consistent with GPS-derived and geological shortening rates, Earth Planet. Sci. Lett., 509, 100–113,
doi:10.1016/j.epsl.2018.12.032, 2019.

Hu, G., Yi, C., Zhang, J., Liu, J., Jiang, T. and Qin, X.: Optically stimulated luminescence dating of a moraine and a terrace in
Laohugou valley, western Qilian Shan, northeastern Tibet, Quat. Int., 321, 37–49, doi:10.1016/j.quaint.2013.12.019, 2014.

Lamb, M. P., Finnegan, N. J., Scheingross, J. S. and Sklar, L. S.: New insights into the mechanics of fluvial bedrock erosion
470 through flume experiments and theory, Geomorphology, 244, 33–55, doi:10.1016/j.geomorph.2015.03.003, 2015.

Meng, X., Zhang, S. and Zhang, Y.: The Temporal and Spatial Change of Temperature and Precipitation in Hexi Corridor in
Recent 57 Years, Acta Geol. Sin., 67(11), 1482–1492, 2012.

Mischke, S., Fuchs, D., Riedel, F. and Schudack, M. E.: Mid to Late Holocene palaeoenvironment of Lake Eastern Juyanze
(north-western China) based on ostracods and stable isotopes, Geobios, 35, 99–110, 2002.

475 Mischke, S., Demske, D., Wünnemann, B. and Schudack, M. E.: Groundwater discharge to a Gobi desert lake during Mid and
Late Holocene dry periods, Palaeogeogr. Palaeoclimatol. Palaeoecol., 225(1–4), 157–172, doi:10.1016/j.palaeo.2004.10.022,
2005.

Pan, B., Burbank, D. W., Wang, Y., Wu, G., Li, J. and Guan, Q.: A 900 k.y. record of strath terrace formation during glacial-interglacial transitions in northwest China, Geology, 31(11), 957–960, doi:10.1130/G19685.1, 2003.

480 Perron, J. T. and Royden, L.: An integral approach to bedrock river profile analysis, Earth Surf. Process. Landforms, 38(6), 570–576, doi:10.1002/esp.3302, 2013.

Raup, B., Racoviteanu, A., Khalsa, S. J. S., Helm, C., Armstrong, R. and Arnaud, Y.: The GLIMS geospatial glacier database: A new tool for studying glacier change, Glob. Planet. Change, 56(1–2), 101–110, doi:10.1016/j.gloplacha.2006.07.018, 2007.

Reimer, P., Bard, E., Bayliss, A., Beck, J., Blackwell, P., Ramsey, C. B., Grootes, P., Guilderson, T., Haflidason, H., Hajdas,

485 I., Hatté, C., Heaton, T., Hoffmann, D., Hogg, A., Hughen, K., Kaiser, K., Kromer, B., Manning, S., Niu, M., Reimer, R., Richards, D., Scott, E., Southon, J., Staff, R., Turney, C. and van der Plicht, J.: IntCal13 and Marine13 Radiocarbon Age Calibration Curves 0–50,000 Years cal BP, Radiocarbon, 55(4), 1869–1887, 2013.

Royden, L. and Perron, J. T.: Solutions of the stream power equation and application to the evolution of river longitudinal profiles, J. Geophys. Res. Earth Surf., 118(2), 497–518, doi:10.1002/jgrf.20031, 2013.

490 Shean, D.: High Mountain Asia 8-meter DEM Mosaics Derived from Optical Imagery, Version 1, tile-224, tile-257, Boulder, Colorado USA. NASA National Snow and Ice Data Center Distributed Active Archive Center, doi:https://doi.org/10.5067/KXOVQ9L172S2, 2017.

Shi, Y.: New Understanding of Quaternary Glaciations in China, Shanghai Popular Science Press, Shanghai (In Chinese)., 2011.

495 Shi, Y., Cui, Z. and Su, Z.: The Quaternary Glaciations and Environmental Variations in China, Hebei Science and Technology Press, Shijiazhuang (In Chinese)., 2006.

Sun, M., Liu, S., Yao, X., Guo, W. and Xu, J.: Glacier changes in the Qilian Mountains in the past half century: Based on the revised First and Second Chinese Glacier Inventory, Acta Geogr. Sin. (In Chinese with English Abstr., 70(9), 1402–1414, doi:10.11821/dlxb201509004, 2015.

500 Tan, L., Cai, Y., Cheng, H., Edwards, L. R., Gao, Y., Xu, H., Zhang, H. and An, Z.: Centennial- to decadal-scale monsoon precipitation variations in the upper Hanjiang River region, China over the past 6650 years, Earth Planet. Sci. Lett., 482, 580–590, doi:10.1016/j.epsl.2017.11.044, 2018.

Tapponnier, P., Xu, Z., Roger, F., Meyer, B., Arnaud, N., Wittlinger, G. and Yang, J.: Oblique stepwise rise and growth of the tibet plateau, Science (80-.)., 294(5547), 1671–1677, doi:10.1126/science.105978, 2001.

505 Tucker, G. E. and Whipple, K. X.: Topographic outcomes predicted by stream erosion models: Sensitivity analysis and intermodel comparison, J. Geophys. Res. Solid Earth, 107(B9), ETG 1-1-ETG 1-16, doi:10.1029/2001JB000162, 2002.

Turowski, J. M., Lague, D. and Hovius, N.: Cover effect in bedrock abrasion: A new derivation and its implications for the modeling of bedrock channel morphology, J. Geophys. Res. Earth Surf., 112(4), doi:10.1029/2006JF000697, 2007.

Wang, Y., Oskin, M. E., Zhang, H., Li, Y., Hu, X. and Lei, J.: Deducing Crustal-Scale Reverse-Fault Geometry and Slip

510 Distribution From Folded River Terraces, Qilian Shan, China, Tectonics, 39(1), 1–18, doi:10.1029/2019TC005901, 2020.

Wei, K. and Gasse, F.: Oxygen isotopes in lacustrine carbonates of West China revisited: Implications for post glacial changes in summer monsoon circulation, Quat. Sci. Rev., 18(12), 1315–1334, doi:10.1016/S0277-3791(98)00115-2, 1999.

Whipple, K. X. and Tucker, G. E.: Dynamics of the stream-power river incision model: Implications for height limits of mountain ranges, landscape response timescales, and research needs, J. Geophys. Res., 3(2), 221–222 [online] Available from:
515   http://dx.doi.org/10.1029/1999JB900120; doi:10.1029/1999JB900120, 1999.

Whittaker, A. C.: How do landscapes record tectonics and climate?, Lithosphere, 4(2), 160–164, doi:10.1130/RF.L003.1, 2012.

Wobus, C., Whipple, K. X., Kirby, E., Snyder, N., Johnson, J., Spyropolou, K., Crosby, B. and Sheehan, D.: Tectonics from topography: Procedures, promise, and pitfalls, Spec. Pap. 398 Tectonics, Clim. Landsc. Evol., 2398(October 2015), 55–74, doi:10.1130/2006.2398(04), 2006.

520   Wohl, E. and David, G. C. L.: Consistency of scaling relations among bedrock and alluvial channels, J. Geophys. Res. Earth Surf., 113(4), 1–16, doi:10.1029/2008JF000989, 2008.

Yang, H., Yang, X., Huang, W., Li, A., Hu, Z., Huang, X. and Yang, H.: 10Be and OSL dating of Pleistocene fluvial terraces along the Hongshuiba River: Constraints on tectonic and climatic drivers for fluvial downcutting across the NE Tibetan Plateau margin, China, Geomorphology, 348, doi:10.1016/j.geomorph.2019.106884, 2020.

525   Zhou, A., Sun, H., Chen, F., Zhao, Y., An, C., Dong, G., Wang, Z. and Chen, J.: High-resolution climate change in mid-late Holocene on Tianchi Lake, Liupan Mountain in the Loess Plateau in central China and its significance, Chinese Sci. Bull., 55(20), 2118–2121, doi:10.1007/s11434-010-3226-0, 2010.